Robotica (2013) volume 31, pp. 123–136. © Cambridge University Press 2012
doi:10.1017/S0263574712000148

Position-singularity analysis of a special class of the Stewart parallel mechanisms with two dissimilar semi-symmetrical hexagons

Baokun Li†,‡, Yi Cao†,§,*, Qiuju Zhang† and Zhen Huang¶

†*School of Mechanical Engineering, Jiangnan University, Wuxi, Jiangsu 214122, China*
‡*School of Mechanical Engineering, Anhui University of Science and Technology, Huainan, Anhui 232001, China*
§*The State Key Laboratory of Fluid Power and Mechatronic Systems, Hangzhou, Zhejiang 310027, China*
¶*Robotics Research Center, Yanshan University, Qinhuangdao, Heibei 066004, China*

(Accepted March 16, 2012. First published online: April 20, 2012)

SUMMARY

In this paper, for a special class of the Stewart parallel mechanism, whose moving platform and base one are two dissimilar semi-symmetrical hexagons, the position-singularity of the mechanism for a constant-orientation is analyzed systematically. The force Jacobian matrix $[\boldsymbol{J}]^T$ is constructed based on the principle of static equilibrium and the screw theory. After expanding the determinant of the simplified matrix $[\boldsymbol{D}]$, whose rank is the same as the rank of the matrix $[\boldsymbol{J}]^T$, a cubic symbolic expression that represents the 3D position-singularity locus of the mechanism for a constant-orientation is derived and graphically represented. Further research shows that the 3D position-singularity surface is extremely complicated, and the geometric characteristics of the position-singularity locus lying in a general oblique plane are very difficult to be identified. However, the position-singularity locus lying in the series of characteristic planes, where the moving platform coincides, are all quadratic curves compromised of infinite many sets of hyperbolas, four pairs of intersecting lines and a parabola. For some special orientations, the quadratic curve can degenerate into two lines or even one line, all of which are parallel to the ridgeline. Two theorems are presented and proved for the first time when the geometric characteristics of the position-singularity curves in the characteristic plane are analyzed. Moreover, the kinematic property of the position-singularity curves is obtained using the Grassmann line geometry and the screw theory. The theoretical results are demonstrated with several numeric examples.

KEYWORDS: Parallel mechanism; Position-singularity; Geometric characteristics; Kinematic property.

1. Introduction

Parallel mechanisms (PMs) have attracted scholars' attention during the past three decades. The popularity has been motivated by the fact that parallel mechanisms have higher stiffness, accuracy, load-carrying capacity, better dynamic performance, and other advantages over serial mechanisms. The Stewart Parallel Mechanism (SPM), which was proposed as a flight simulator in 1965,[1] is one of the best well-known PMs, and now is widely used in many other applications, such as docking mechanism of the aircrafts, parallel kinematic machines, medical micromanipulators, satellite antennas, and micro- and nano-scale precision position systems.[2]

One important concern of PMs is the singular configuration, on which the end-effector gains one or more unwanted instantaneous degrees of freedom (DOFs) even if all the actuators are locked. Such situation can transitorily make the drive force go infinity, and then put the PM out of control. Many researchers have paid attention to this phenomenon. Hunt[3] first discovered the singular configuration for the SPM that occurs when all the segments associated with prismatic actuators intersect a common line. Fichter[4] pointed out that a singular configuration of the 3/6-SPM occurs when the moving platform parallel to the base one and rotate around the vertical axis by $\pm 90^\circ$. The 3/6-SPM has one triangular moving platform and one hexagonal base platform. Merlet[5–7] studied systematically the singularity of the 3/6-SPM using the Grassmann line geometry, including types of 3c, 4b, 4d, 5a, and 5b. Gosselin and Angeles[8] showed that the singularities of PMs could be classified into three types based on the determinants of the PMs' Jacobian matrices. This classification was refined by Zlatanov *et al.*[9] Ma and Angeles[10] researched the architecture singularities of the PMs. Huang and coworkers[11–13] explored the kinematics principle of PMs, and proposed a new sufficient and necessary condition to determine the singularity of PMs. Pendar *et al.*[14] introduced a geometrical method to obtain the singular configuration based on the famous Ceva plane geometry theorem. The methods proposed in refs. [11–14] are very effective to analyze the singularities of the class of 3/3-SPM and 3/6-SPM, which have triangular moving platform. Saglia and Dai[15] proposed that the singularity of the parallel mechanism could be eliminated using the redundant actuators. Zhu *et al.*[16] illustrated the singularity of the fully symmetrical 5-DOF 3R2T PM based on the screw theory and the Grassmann line geometry. Ben-Horin and Shoham[17] obtained an algebra statement to analyze the singularity of a class of SPMs using the Grassmann–Cayley algebra.

Owing to Li *et al.*,[18] it is desirable for designers to obtain the analytical expression and have a graphical

* Corresponding author. Email: caoyi@jiangnan.edu.cn

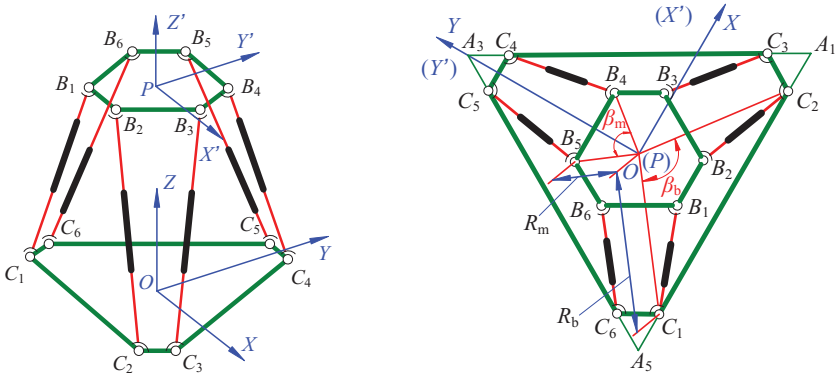

Fig. 1. (Colour online) Sketch of the special class of SPM.

representation of the singularity locus of a PM. In this case, it is easy to identify the locations of singularities within the given workspace and determine whether the singularity can be avoided. Sefrioui and Gosselin[19,20] studied the singularity loci of the planar and spherical PMs. Then Wang and Gosselin[21] obtained the singularity loci of spatial 4-DOF PMs. For the class of 6-DOF SPMs, the singularity expression was derived by several researchers. St-Onge and Gosselin[22] pointed out that the singularity locus equation of the general SPM should be a polynomial expression of degree three, and also studied the graphical representation of the singularity locus. For the 3/6-SPM, Huang *et al.*[23] transformed the complicated singularity analysis into a simpler position analysis of a planar mechanism by proposing a planar singularity-equivalent mechanism based on the kinematic principle of singularity introduced in refs. [11–13], and the polynomial expression of degree three representing the singularity locus for a constant-orientation was derived. Huang and Cao[24] derived a cubic singularity expression for a constant-orientation of the 6/6-SPM, whose moving platform and base one are two semi-symmetrical hexagons. Bandyopadhyay and Ghosal[25] also obtained the singularity manifold of the 6/6-SPM as a cubic surface in^3, and further showed that the cubic surface in the sections, which is parallel to the base platform of the mechanism, is a quadratic curve. Cheng *et al.*[26] gave graphical representations of the position-singularity loci for different constant-orientations and the orientation-singularity loci at different positions based on unit quaternion as orientation parameters, but did not obtain general expressions of position-singularity and orientation-singularity. Nawratil[27] proposed a set of specific types of SPMs, which possess non-cubic singularity surface for orientation.

For a special class of SPMs, whose moving platform and base one are two dissimilar semi-symmetrical hexagons, the geometric characteristics and kinematic property of the singularity loci have not been studied. This paper focuses on this research area, and its context is briefly as follows: In Section 2, the geometry of this special class of SPMs is described. In Section 3, the force Jacobian matrix is constructed using the principle of static equilibrium and the screw theory, and the method of determining the unwanted instantaneous screw motion when the mechanism is singular is introduced. In Section 4, after expanding the determinant, the matrix $[\boldsymbol{D}]$, whose rank is the same as the rank of the force Jacobian matrix $[\boldsymbol{J}]^T$, a cubic symbolic expression that represents the position-singularity locus of the mechanism for a constant-orientation is obtained. And then the 3D position-singularity surfaces of the mechanism with given geometry parameters for several orientations are graphically represented. In Section 5, a quadratic symbolic expression representing the position-singularity curve lying in the characteristic plane, which coincides with the moving platform, is derived after setting a new special coordinate system and using the coordinate transformation. Then the geometric characteristics of the position-singularity curve in the characteristic plane are further discussed based on the theory of analytic plane geometry. In particular, two theorems are presented and proved for the first time when the geometric characteristics of the position-singularity curve are analyzed. Moreover, the kinematic property of the position-singularity curve is also investigated using the screw theory and the Grassmann line geometry. Finally, some meaningful conclusions are reached and the future work is presented.

2. Geometry of the SPM with Two Dissimilar Semi-Symmetrical Hexagons

The sketch of this special class of SPM is shown in Fig. 1. The mechanism consists of a moving platform and a base one connected via six identical SPS or SPU legs $(B_iC_i)(i = 1, 2, \ldots, 6)$. Here, S denotes a spherical joint and U denotes a Hooke joint which are passive, while P denotes an actuated prismatic joint. The moving platform and the base one, whose vertices are B_i and $C_i(i = 1, 2, \ldots, 6)$, respectively, are both semi-symmetrical hexagons but dissimilar with each other. $A_j(j = 1, 3, 5)$ are the intersection points of the longer sides of the base platform. $P(O)$, $\beta_{\mathrm{m}}(\beta_{\mathrm{b}})$, $R_{\mathrm{m}}(R_{\mathrm{b}})$ are the geometrical center, the central angle of the side B_4B_5 (C_1C_2), and the circumradius of the moving (base) platform, respectively, where $\beta_{\mathrm{m}} \neq \beta_{\mathrm{b}}$ and $\beta_{\mathrm{m}} + \beta_{\mathrm{b}} \neq 120^\circ$ considering that the moving platform and the base one are two dissimilar hexagons. Without loss of generality, the length here is non-dimensional. Finally, the geometry of the mechanism is defined by four parameters (R_{m}, R_{b}, β_{m}, and β_{b}).

3. The Force Jacobian Matrix and the Unwanted Instantaneous Screw Motion

The moving reference frame *P-X'Y'Z'* and the fixed one *O-XYZ* are attached to the moving platform and the base

https://doi.org/10.1017/S0263574712000148 Published online by Cambridge University Press

platform, respectively. The coordinates of six vertices, $B_i (i = 1, 2, \ldots, 6)$, of the moving platform are denoted as $\boldsymbol{B}'_i(B'_{iX}, B'_{iY}, B'_{iZ})$ $(i = 1, 2, \ldots, 6)$ with respect to the moving reference frame and as $\boldsymbol{B}_i(B_{iX}, B_{iY}, B_{iZ})(i = 1, 2, \ldots, 6)$ with respect to the fixed reference frame. Similarly, $\boldsymbol{C}_i(C_{iX}, C_{iY}, C_{iZ})(i = 1, 2, \ldots, 6)$ represents the coordinates of vertices $C_i (i = 1, 2, \ldots, 6)$ with respect to the fixed reference frame. The coordinates $\boldsymbol{B}'_i, \boldsymbol{C}_i (i = 1, 2, \ldots, 6)$ are shown in Appendix A. The coordinates of point P with respect to the fixed reference frame are designated as $\boldsymbol{P}(X, Y, Z)$. Here the standard *Z-Y-Z*-Euler angles (ϕ, θ, ψ) are used to represent the orientation of the moving platform. Thus, the ridgeline, which is the intersecting line of the moving plane *X'–P–Y'* and the fixed plane *X-O-Y* can be located[2] and is described in Section 5.1.

The relation between $\boldsymbol{B}_i$ and $\boldsymbol{B}'_i (i = 1, 2, \ldots, 6)$ satisfies

$$\begin{bmatrix} B_{iX} \\ B_{iY} \\ B_{iZ} \end{bmatrix} = [\boldsymbol{R}] \begin{bmatrix} B'_{iX} \\ B'_{iY} \\ B'_{iZ} \end{bmatrix} + \begin{bmatrix} X \\ Y \\ Z \end{bmatrix}, \tag{1}$$

where the matrix $[\boldsymbol{R}]$ is the rotation matrix of the moving reference frame to the fixed platform using the standard *Z-Y-Z*-Euler angles to represent the orientation of the moving platform. And then the force Jacobian matrix of the mechanism can be constructed according to the principle of static equilibrium and the screw theory[11]:

$$[\boldsymbol{J}]^T = \begin{bmatrix} \boldsymbol{S}_1 & \boldsymbol{S}_2 & \boldsymbol{S}_3 & \boldsymbol{S}_4 & \boldsymbol{S}_5 & \boldsymbol{S}_6 \\ \boldsymbol{S}_{01} & \boldsymbol{S}_{02} & \boldsymbol{S}_{03} & \boldsymbol{S}_{04} & \boldsymbol{S}_{05} & \boldsymbol{S}_{06} \end{bmatrix}, \tag{2a}$$

$$[\boldsymbol{J}]^T = \begin{bmatrix} \dfrac{\boldsymbol{B}_1 - \boldsymbol{C}_1}{|\boldsymbol{B}_1 - \boldsymbol{C}_1|} & \dfrac{\boldsymbol{B}_2 - \boldsymbol{C}_2}{|\boldsymbol{B}_2 - \boldsymbol{C}_2|} & \dfrac{\boldsymbol{B}_3 - \boldsymbol{C}_3}{|\boldsymbol{B}_3 - \boldsymbol{C}_3|} & \dfrac{\boldsymbol{B}_4 - \boldsymbol{C}_4}{|\boldsymbol{B}_4 - \boldsymbol{C}_4|} & \dfrac{\boldsymbol{B}_5 - \boldsymbol{C}_5}{|\boldsymbol{B}_5 - \boldsymbol{C}_5|} & \dfrac{\boldsymbol{B}_6 - \boldsymbol{C}_6}{|\boldsymbol{B}_6 - \boldsymbol{C}_6|} \\ \dfrac{\boldsymbol{C}_1 \times \boldsymbol{B}_1}{|\boldsymbol{B}_1 - \boldsymbol{C}_1|} & \dfrac{\boldsymbol{C}_2 \times \boldsymbol{B}_2}{|\boldsymbol{B}_2 - \boldsymbol{C}_2|} & \dfrac{\boldsymbol{C}_3 \times \boldsymbol{B}_3}{|\boldsymbol{B}_3 - \boldsymbol{C}_3|} & \dfrac{\boldsymbol{C}_4 \times \boldsymbol{B}_4}{|\boldsymbol{B}_4 - \boldsymbol{C}_4|} & \dfrac{\boldsymbol{C}_5 \times \boldsymbol{B}_5}{|\boldsymbol{B}_5 - \boldsymbol{C}_5|} & \dfrac{\boldsymbol{C}_6 \times \boldsymbol{B}_6}{|\boldsymbol{B}_6 - \boldsymbol{C}_6|} \end{bmatrix}, \tag{2b}$$

where $\$_i^r = (\boldsymbol{S}_i; \boldsymbol{S}0i) = (L_i, M_i, N_i; P_i, Q_i, R_i)(i = 1, 2, \ldots, 6)$ are the Plücker coordinates of the vertex of the *i*th limb.

As $|\boldsymbol{B}_i - \boldsymbol{C}_i|$ is the length of the *i*th limb, and is non-zero, the force Jacobian matrix $[\boldsymbol{J}]^T$ and the following matrix $[\boldsymbol{D}]$, written as Eq. (3), have the same rank,

$$[\boldsymbol{D}] = \begin{bmatrix} \boldsymbol{B} - \boldsymbol{C}_1 & \boldsymbol{B}_2 - \boldsymbol{C}_2 & \boldsymbol{B}_3 - \boldsymbol{C}_3 & \boldsymbol{B}_4 - \boldsymbol{C}_4 & \boldsymbol{B}_5 - \boldsymbol{C}_5 & \boldsymbol{B}_6 - \boldsymbol{C}_6 \\ \boldsymbol{C}_1 \times \boldsymbol{B}_1 & \boldsymbol{C}_2 \times \boldsymbol{B}_2 & \boldsymbol{C}_3 \times \boldsymbol{B}_3 & \boldsymbol{C}_4 \times \boldsymbol{B}_4 & \boldsymbol{C}_5 \times \boldsymbol{B}_5 & \boldsymbol{C}_6 \times \boldsymbol{B}_6 \end{bmatrix}. \tag{3}$$

The mechanism is singular when the determinant of the Jacobian matrix $[\boldsymbol{J}]^T$ is zero. As the matrix $[\boldsymbol{D}]$ and the force Jacobian matrix $[\boldsymbol{J}]^T$ have the same rank, the determinant of the matrix $[\boldsymbol{D}]$ can be used as the discriminant of the singularity. For most of the singularities of the 6/6-SPM, the rank of the force Jacobian matrix $[\boldsymbol{J}]^T$ is five, then an unwanted DOF, which is an instantaneous screw motion $\$^m$ with pitch h^m, can be derived as follows[11]:

$$\$^m = \begin{vmatrix} \in i & \in j & \in k & i & j & k \\ L_1 & M_1 & N_1 & P_1 & Q_1 & R_1 \\ L_2 & M_2 & N_2 & P_2 & Q_2 & R_2 \\ L_3 & M_3 & N_3 & P_3 & Q_3 & R_3 \\ L_4 & M_4 & N_4 & P_4 & Q_4 & R_4 \\ L_5 & M_5 & N_5 & P_5 & Q_5 & R_5 \end{vmatrix}, \tag{4}$$

where $\$^m$ is reciprocal to $\$_i^r$, and can also be expressed as a dual vector. After expanding, Eq. (4), the unwanted instantaneous screw motion $\$^m$ can be deduced:

$$\left(\boldsymbol{S}^m; \boldsymbol{S}_0^m\right) = (L^m, M^m, N^m; P^m, Q^m, R^m),$$

where L^m, M^m, N^m, P^m, Q^m, and R^m are the coefficients of $i, j, k, \in i, \in j, \in k$, respectively. The pitch h^m of the screw motion $\$^m$ can be calculated using the following equation:

$$h^m = (L^m P^m + M^m Q^m + N^m R^m)/(L^{m^2} + M^{m^2} + N^{m^2}). \tag{5}$$

4. The 3D Position-Singularity Locus

Based on determinants of the mechanism's Jacobian matrices, Gosselin and Angeles[8] showed that singularities of PMs could be classified into three different types: inverse kinematic singularity, direct kinematic singularity, and architecture singularity. For the first type of singularity occurring when different branches of inverse kinematics problem converge, i.e. the determinant of the Jacobian matrix $[\boldsymbol{J}]$ of this special class of SPMs being equal to infinity, i.e. $\det([\boldsymbol{J}]) = \infty$, where symbol ∞ denotes infinity. It is easy to deal with it, since it leads to a very simple expression. Therefore, the inverse kinematic singularity analysis of this special class of SPMs will not be addressed here. For more and complete descriptions of the inverse kinematic singularity analysis of this class of SPMs, we refer the reader to the detailed explanations given by St-Onge and Gosselin.[22] For the third type of singularity, when $\beta_m + \beta_b = 120^\circ$, the moving platform and the base one are two similar hexagons and the corresponding points are connected, then the mechanism is architecture singularity. In this case, whatever is the pose of the GSPM, the mechanism is in singularity. For the second type of singularity occurring when different branches of the direct kinematics problem converge, it is difficult to analyze and has received much attention from many researchers. This paper will only deal with the direct

https://doi.org/10.1017/S0263574712000148 Published online by Cambridge University Press

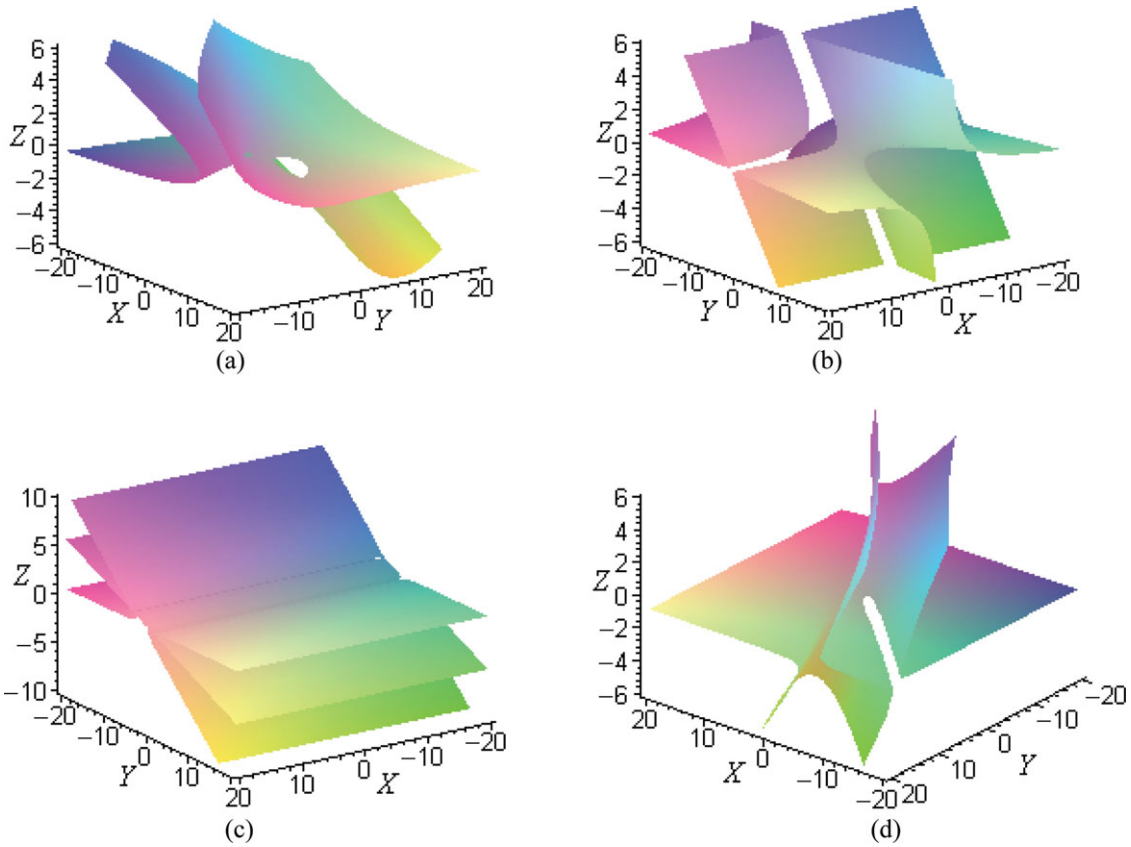

Fig. 2. (Colour online) Position-singularity loci for different orientations: (a) Orientation (60°, 30°, −45); (b) orientation (90°, 30°, 0); (c) orientation (90°, 30°, −90°); and (d) orientation (45°, 60°, −30°).

kinematic singularity analysis of this special class of SPMs that occurs when the determinant of the Jacobian matrix $[\boldsymbol{J}]$ is equal to zero, i.e. $\det([\boldsymbol{J}]) = 0$. The Jacobian matrix $[\boldsymbol{J}]$ here is the transpose of the force Jacobian matrix $[\boldsymbol{J}]^T$ as presented in Section 3.

Substituting Eq. (1) into Eq. (3), expanding and rearranging the determinant of the matrix $[\boldsymbol{D}]$, which is equal to zero when the mechanism is singular, yields a cubic symbolic expression involving the variables (X, Y, Z). The expression representing the position-singularity locus for a constant-orientation (ϕ, θ, ψ) can be written as the following equation:

$$f_1Z^3 + f_2XZ^2 + f_3YZ^2 + f_4X^2Z + f_5Y^2Z + f_6XYZ + f_7Z^2 + f_8XZ + f_9YZ + f_{10}X^2 + f_{11}XY + f_{12}Y^2 + f_{13}Z + f_{14}X + f_{15}Y + f_{16} = 0, \tag{6}$$

where $f_i (i = 1, 2, \ldots, 16)$ are all functions involving the geometry parameters R_{m}, R_{b}, β_{m}, and β_{b}, and the orientation parameters (ϕ, θ, ψ). The graphical representations of the position-singularity loci for several different orientations are shown in Fig. 2. The geometry parameters here are given as $R_{\mathrm{m}} = 1$, $R_{\mathrm{b}} = 2$, $\beta_{\mathrm{m}} = 75°$, and $\beta_{\mathrm{b}} = 105°$.

Figure 2 shows that the graphical representations of the position-singularity surfaces of the mechanism for different orientations are all rather complicated and quite variable.

The symbolic expression and surfaces of the position-singularity developed here are of great importance for the design and analysis of the mechanism. They allow the designers to visualize the singularity surface within the workspace for a given orientation and conclude whether and how the singularity can be avoided.

5. Analysis of the Position-Singularity Locus in the Characteristic Plane

5.1. Position-singularity locus in the characteristic plane

The configuration of the mechanism for a constant-orientation (ϕ, θ, ψ), where $\theta \neq 0$, is briefly shown in Fig. 3. The moving plane *X'-P-Y'* in which the moving platform lies is called the characteristic plane, and the plane *X-O-Y* in which the base platform lies is defined as the base plane. The intersection angle between the characteristic plane and the base plane is θ. When θ is non-zero, the characteristic plane is not parallel to the base plane. Points *U*, *V*, and *W* are the intersecting points of the ridgeline and the three sides C_5C_6, C_3C_4, and C_1C_2, respectively. A new moving reference frame *V-xy* is set in the characteristic plane. The coordinates of the point *V* with respect to the fixed reference frame *O-XYZ* is denoted as $\boldsymbol{V}(X_{\mathrm{v}}, Y_{\mathrm{v}}, 0)$. Then the position of the characteristic plane is determined by angle θ and the coordinates $\boldsymbol{V}(X_{\mathrm{v}}, Y_{\mathrm{v}}, 0)$, where Y_{v} can be established as

$$Y_{\mathrm{v}} = 2R_b \cos(\beta_{\mathrm{b}}/2) - \sqrt{3}X_{\mathrm{v}}. \tag{7}$$

The equation of line *UV* in the fixed plane with respect to the plane-coordinate system *O-XY* can be written as

https://doi.org/10.1017/S0263574712000148 Published online by Cambridge University Press

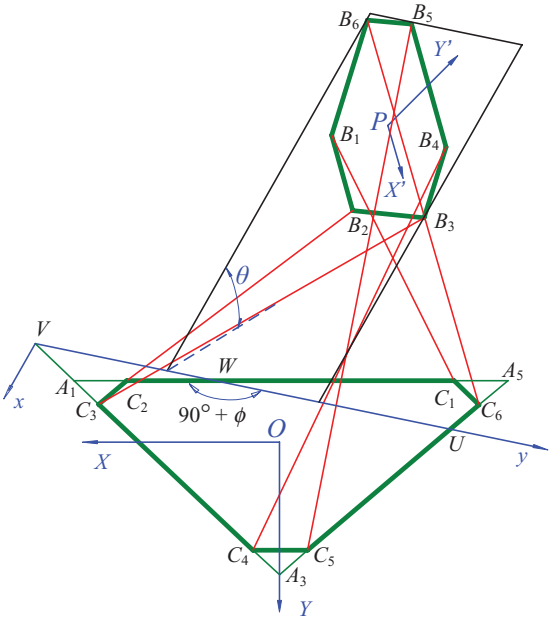

Fig. 3. (Colour online) Configuration of the mechanism for a constant-orientation.

follows:

$$Y - 2R_b \cos(\beta_b/2) + \sqrt{3}X_v = -\cot(\phi)(X - X_v). \quad (8)$$

Synthesizing Eq. (8) and the equations of lines C_5C_6, C_3C_4, and C_1C_2 with respect to the plane-coordinate system O-XY, the coordinates of points U, V, and W can be obtained. Besides, the equations of lines C_5C_6, C_3C_4, and C_1C_2 with respect to the plane-coordinate system O-XY can easily be deduced according to the geometry of the mechanism.

The meaning of (X, Y, Z) has been defined in Section 3, and (x, y) denotes the coordinates of point P with respect to the moving reference frame V-xy. These satisfy Eq. (9):

$$\begin{aligned} X &= x\cos\phi\cos\theta - y\sin\phi + X_v, \\ Y &= x\sin\phi\cos\theta + y\cos\phi + Y_v \ , \\ Z &= -x\sin\theta. \end{aligned} \quad (9)$$

The substitution of Eq. (9) into Eq. (6) with noting Eq. (8) leads to a symbolic expression, which can be deduced as Eq. (10) after rearrangements. The symbolic expression written as Eq. (10) describes the position-singularity locus of the mechanism in the characteristic plane:

$$\sin^3\theta(ax^2 + 2bxy + cy^2 + 2dx + 2ey + f) = 0. \quad (10)$$

Since θ is non-zero, the position-singularity locus in the characteristic plane becomes

$$ax^2 + 2bxy + cy^2 + 2dx + 2ey + f = 0, \quad (11)$$

where the coefficient c is identically equal to zero, and the coefficients a, b, d, e, and f are all functions of the geometry parameters R_m, R_b, β_m, and β_b, the Euler angles (ϕ, ψ), and X_v. Equation (11) is an expression of quadratic curve with respect to x and y, and irrespective of θ.

It must be pointed out that the aforementioned results do not consider the special case that the orientation of the moving platform is (30°, θ, ψ) or (−150°, θ, ψ), where the ridgeline is parallel to the line C_3C_4, which means that the ridgeline intersects the line C_3C_4 at infinite distance. In this special case, the origin of the coordinate system V-xy can be set as point W. Then the position-singularity expression in the characteristic plane can also be derived using the method that is similar to the aforementioned method. Then it can be demonstrated that the position-singularity expression in the characteristic plane expressed as Eq. (11) also holds for the orientation (30°, θ, ψ) or (−150°, θ, ψ).

Therefore, we can conclude that the 3D position-singularity expression for a constant-orientation of mechanism is a cubic polynomial. Figure 2 shows that the 3D position-singularity surfaces for different orientations are very complex and diverse. However, the substitution of Eq (9) into Eq (6) can obtain a quadratic expression, which represents a 2D position-singularity curve in a characteristic plane where the moving platform lies. It can also be shown that the nature of position-singularity for a constant-orientation obtained here is the same as illustrated by ref. 23. However, it should be indicated that as the class of SPMs with two similar semi- symmetrical hexagons, which was proposed in ref. [23], can be regarded as a specific geometric configuration of the types of SPMs with two dissimilar semi-symmetrical hexagons proposed in this paper, the investigation here has more generalities than discussed in ref. 23.

The intersecting curve between the position-singularity locus and a general oblique plane is always an extremely complicated cubic expression and difficult to be characterized. For example, when $R_a = 2$, $R_b = 1$, $\beta_b = 105°$, $\beta_m = 75°$, and $(\phi, \theta, \psi) = (60°, 30°, -45°)$, the intersecting curve between the position-singularity locus and the planes, $Z = X/3$ and $Z = X/2 - 3Y/5 + 3/4$, are expressed as Eqs. (12a) and (12b):

$$\begin{aligned} &376X^3 - (1200\sqrt{3} - 2520)X^2Y - (1224\sqrt{3} \\ &\quad - 2232)XY^2 - (57\sqrt{2} - 1046\sqrt{3} + 1689 \\ &\quad - 54\sqrt{6})t_1X^2 - (828\sqrt{2} - 495\sqrt{6} + 2556 \\ &\quad -1479\sqrt{3})t_1XY - (585\sqrt{2} - 339\sqrt{6} + 2376 \\ &\quad -1212\sqrt{3})X - (1476\sqrt{3} + 837\sqrt{6} - 2592 - 1377\sqrt{2})Y \\ &\quad -(837\sqrt{6} - 6102 + 3510\sqrt{3} - 1377\sqrt{2})t_1 = 0 \end{aligned} \quad (12a)$$

$$\begin{aligned} &36000X^3 - (44400 + 14000\sqrt{3})X^2Y - (6720 \\ &\quad -23040\sqrt{3})XY^2 - (7488\sqrt{3} - 9792)Y^3 + (1000\sqrt{6}t_1 \\ &\quad -54000t_1 - 15000\sqrt{3} + 35000\sqrt{3}t_1 + 153000)X^2 \\ &\quad -(61200 + 58300\sqrt{3}t_1 - 8100\sqrt{6}t_1 + 14100\sqrt{2}t_1 \\ &\quad -93900t_1 + 51600\sqrt{3})XY + (26760\sqrt{3}t_1 - 3960\sqrt{6}t_1 \\ &\quad -83520 + 6840\sqrt{2}t_1 + 67680\sqrt{3} - 45000t_1)Y^2 \\ &\quad -(8250\sqrt{6}t_1 - 15750\sqrt{2}t_1 + 4000\sqrt{6} + 164250t_1 \\ &\quad -102000 - 99750\sqrt{3}t_1 - 15000\sqrt{3} - 6000\sqrt{2})X \\ &\quad +(123750t_1 + 34650\sqrt{6}t_1 - 59850\sqrt{2}t_1 + 19200\sqrt{6} \\ &\quad -32400\sqrt{2} + 195300 - 72150\sqrt{3}t_1 - 142700\sqrt{3})Y \\ &\quad +(375\sqrt{3} + 82125\sqrt{2} - 49125\sqrt{6} - 375)t_1 - 39000\sqrt{6} \\ &\quad -87750 + 62250\sqrt{3} + 63000\sqrt{2} = 0 \end{aligned} \quad (12b)$$

https://doi.org/10.1017/S0263574712000148 Published online by Cambridge University Press

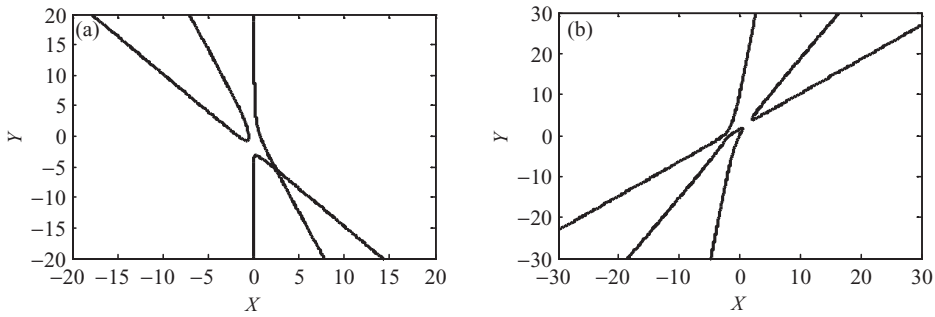

Fig. 4. Intersecting curves in the two general oblique planes: (a) in the plane $Z = X/3$; (b) in the plane $Z = X/2 - 3Y/5 + 3/4$.

where $t_1 = \sqrt{8 + 2\sqrt{6} - 2\sqrt{2}}$ (the same below). It can be shown that neither of these two equations can be factorized. Figure 4 shows the curves that are described by Eqs. (12a) and (12b).

With the above description, it is difficult to characterize the position-singularity curve in a general oblique plane, but easy to do it in the characteristic plane. That is why the moving plane *X'-P-Y'*, where the moving platform lies, is called the characteristic plane.

5.2. Analysis of the geometric characteristics and kinematic property of the position-singularity locus

The geometric characteristics of the position-singularity locus in the characteristic plane can be analyzed by two invariants:

$$\delta = \begin{vmatrix} a & b \\ b & c \end{vmatrix} = ac - b^2 = -b^2, \tag{13a}$$

$$\Delta = \begin{vmatrix} a & b & d \\ b & c & e \\ d & e & f \end{vmatrix} = -ae^2 - b^2 f + 2bde. \tag{13b}$$

According to the theory of the analytic plane geometry, the values of δ and Δ indicate the geometric characteristics of the quadratic curve. The characteristics of the quadratic position-singularity curve in the characteristic plane for any given geometry parameters and orientation parameters mainly have the following four cases:

Case 1. $\delta < 0$ and $\Delta \neq 0$, Eq. (11) represents an expression of a set of hyperbolas.

Case 2. $\delta < 0$ and $\Delta = 0$, Eq. (11) can be factorized into product of two polynomial expressions of degree one. Then Eq. (11) describes a pair of intersecting lines, which are the degeneration of hyperbolas.

Case 3. $\delta = 0$ and $\Delta \neq 0$, Eq. (11) is an expression of a parabola.

Case 4. $\delta = 0$ and $\Delta = 0$, there are two cases: Firstly, when $d^2 - af > 0$, Eq. (11) designates into two parallel lines. Secondly, when $d^2 - af = 0$, the two parallel lines become one line.

Further research shows that the coefficients a, b, and e of Eq. (11) are all polynomial expressions of degree one with respect to X_v, and the coefficients d and f are both quadratic with respect to X_v. In addition, it can be concluded that the maximum degree of X_v is four in the invariant Δ. Thus, equation $\delta = 0$, i.e. $b = 0$, has one root for X_v, and equation $\Delta = 0$ has four roots for X_v. In particular, when $\phi = \pm 90^\circ$ and $\psi = 0^\circ$, both a and e are identically vanishing, and when $\phi = \pm 90^\circ$ and $\psi = \pm 90^\circ$, both b and e are identically vanishing.

With above presentations, Eq. (11) generally represents in infinity many sets of hyperbolas. Other three cases should be considered as follows: Firstly, four values of X_v satisfy equation $\Delta = 0$, so the sets of hyperbolas can degenerate into four pairs of intersecting lines. Secondly, noting that only one value of X_v satisfies equation $\delta = 0$, i.e. $b = 0$, Eq. (11) consequently describes only one parabola. Further, the fact that the symmetry axis of the parabola must be parallel to the y-axis, i.e. the ridgeline is easy to be achieved. Finally, when $(\phi, \psi) = (\pm 90^\circ, \pm 90^\circ)$, since b and e are both identically vanishing, Eq. (11) becomes two parallel lines, even one line which is parallel to the y-axis, i.e. the ridgeline.

Theorem 1. If the position-singularity locus of the mechanism for a constant-orientation in the characteristic plane is a set of hyperbolas, the equations of two asymptotes, one of which must be parallel to the ridgeline, i.e. the y-axis of the coordinate system *V-xy*, can be written as follows:

$$x = -e/b, \tag{14a}$$

$$abx + 2b^2 y + 2bd - ae = 0. \tag{14b}$$

Proof. When $a \neq 0$, translate the origin of the plane-coordinate system *V-xy* in the characteristic plane into the central point of the hyperbola, and then rotate the coordinate system *V'-x'y'* by an angle of α around the central point, whose coordinates in the coordinate system *V-xy* are denoted by (x_0, y_0):

$$x_0 = \frac{be - cd}{\delta} = -\frac{e}{b}, \quad y_0 = \frac{bd - ae}{\delta} = -\frac{bd - ae}{b^2}. \tag{15}$$

The value of α is determined by two equations described as follows:

$$\sin 2\alpha = \frac{2b}{\sqrt{(2b)^2 + (a - c)^2}}, \tag{16a}$$

$$\cos 2\alpha = \frac{a - c}{\sqrt{(2b)^2 + (a - c)^2}}. \tag{16b}$$

https://doi.org/10.1017/S0263574712000148 Published online by Cambridge University Press

Using Eqs. (16a) and (16b) yields

$$\tan\alpha = \frac{-a+\sqrt{a^2+4b^2}}{2b}. \tag{17}$$

The equation of hyperbolas expressed as Eq. (11) can be transformed into the standard form:

$$a'x'^2 + c'y'^2 + \frac{\Delta}{\delta} = 0, \tag{18}$$

where

$$a' = \frac{a+c+\sqrt{(a-c)^2+4b^2}}{2} = \frac{a+\sqrt{a^2+4b^2}}{2},$$
$$c' = \frac{a+c-\sqrt{(a-c)^2+4b^2}}{2} = \frac{a-\sqrt{a^2+4b^2}}{2}.$$

The slopes of two asymptotes of hyperbolas in the new coordinate system *V'-x'y'* are

$$k_1' = \tan\beta_1' = \sqrt{-\frac{a'}{c'}} = \sqrt{-\frac{a+\sqrt{a^2+4b^2}}{a-\sqrt{a^2+4b^2}}}$$
$$= \frac{a+\sqrt{a^2+4b^2}}{2b}, \tag{19a}$$
$$k_2' = \tan\beta_2' = -\sqrt{-\frac{a'}{c'}} = -\sqrt{-\frac{a+\sqrt{a^2+4b^2}}{a-\sqrt{a^2+4b^2}}}$$
$$= -\frac{a+\sqrt{a^2+4b^2}}{2b}. \tag{19b}$$

Then the slope of one of the two asymptotes of hyperbolas in the original coordinate system *V-xy* can be obtained using the trigonometric formula:

$$k_1 = \tan(\alpha+\beta_1') = \frac{\tan\alpha+\tan\beta_1'}{1-\tan\alpha\tan\beta_1'} = \frac{\tan\alpha+\tan\beta_1'}{0} = \infty. \tag{20a}$$

The slope of another asymptote is

$$k_2 = \tan(\alpha+\beta_2') = \frac{\tan\alpha+\tan\beta_2'}{1-\tan\alpha\tan\beta_2'} = -\frac{a}{2b}. \tag{20b}$$

This means that the point-slope equations of two asymptotes of hyperbolas in the original coordinate system *V-xy* can be deduced as follows:

$$x = -e/b, \tag{21a}$$

$$y + \frac{bd-ae}{b^2} = -\frac{a}{2b}\left(x+\frac{e}{b}\right). \tag{21b}$$

Eq. (21b) can be written in another form after rearrangement:

$$abx + 2b^2y + 2bd - ae = 0. \tag{22}$$

When $a = 0$, Eq. (11) becomes

$$2bxy + 2dx + 2ey + f = 0. \tag{23}$$

Eq. (23) is equivalent to the following equation:

$$(bx+e)\left(y+\frac{d}{b}\right) = \frac{2de-bf}{2b}. \tag{24}$$

It also represents an equation of a set of hyperbolas. Equations of two asymptotes of hyperbolas described as Eq. (24) can be written as follows:

$$x = -e/b, \tag{25a}$$

$$y = -d/b. \tag{25b}$$

Eq. (25a) is equivalent to Eq. (14a). Besides, when $a = 0$, Eq. (14b) can be simplified as Eq. (25b). Therefore, Eqs. (14a) and (14b) can hold for any value of a.

It can be concluded from Theorem 1 that the position-singularity locus of the mechanism for a constant-orientation in the characteristic plane is a set of hyperbolas, and one of the two asymptotes of hyperbolas must be parallel to the *y*-axis of the coordinates system *V-xy*, i.e. the ridgeline.

Theorem 2. If the position-singularity locus of the mechanism for a constant-orientation in the characteristic plane is a pair of intersecting lines, one of the two lines must be parallel to the ridgeline, i.e. the *y*-axis of the coordinate system *V-xy*. The forms of these two intersecting lines and the forms of two asymptotes of hyperbolas are same.

Proof. Theorem 2 can be proved using the method of undetermined coefficients. The procedure is demonstrated as follows:

When $\delta < 0$ and $\Delta = 0$, Eq. (11) represents a pair of intersecting lines. Noting $c \equiv 0$, Eq. (11) can be factorized into the product of two polynomial expressions with respect to x and y:

$$(x+B)(Ax+Cy+D) = 0. \tag{26}$$

Expanding Eq. (26) leads to

$$Ax^2 + Cxy + (AB+D)x + BCy + BD = 0. \tag{27}$$

After comparing Eq. (27) with Eq.(11), the following equations set can be obtained:

$$\begin{aligned} A &= a \\ C &= 2b \\ AB+D &= 2d \\ BC &= 2e \\ BD &= f \end{aligned}. \tag{28}$$

Equation (28) can be solved and the solutions can be deduced: $A = a$, $B = e/b$, $C = 2b$, $D = bf/e$. Substituting these solutions into Eq. (26) yields

$$\left(x+\frac{e}{b}\right)\left(ax+2by+\frac{bf}{e}\right) = 0. \tag{29}$$

https://doi.org/10.1017/S0263574712000148 Published online by Cambridge University Press

Table I. Cases of the first SLCS of hyperbolas.

X_v	(x, y)	$\$^m$
1	(0.4810565, 1.4875392)	(0.4157354, −0.9044200, 0.0958566; 0.4217756, 0.0912636, −0.9681797)
	(1.4331802, −3.6995819)	(0.0390977, 0.9790733, −0.1997167; 0.3796017, 0.5529974, 2.7852780)
	(3.4429472, −2.4797896)	(0.8668142, 0.4289855, −0.2541743; 0.3633554, −0.8000619, −0.1111575)
2	(0.0127256, 1.2353741)	(0.4157354, −0.9044200, 0.0958566; 0.4217756, 0.0912636, −0.9681797)
	(0.6672951, −2.8412510)	(0.0390977, 0.9790733, −0.1997167; 0.3796017, 0.5529974, 2.7852780)
	(2.0489770, 0.7225780)	(0.8668142, 0.4289855, −0.2541743; 0.3633554, −0.8000619, −0.1111575)

It can be expanded to

$$ax^2 + 2bxy + \left(\frac{bf}{e} + \frac{ae}{b}\right)x + 2ey + f = 0. \qquad (30)$$

Note $\Delta = -b^2 f - ae^2 + 2bde = 0$, so

$$\frac{bf}{e} + \frac{ae}{b} = 2d. \qquad (31)$$

Therefore, when $\Delta = 0$, Eq. (29) is equivalent to Eq. (11) and represents a pair of intersecting lines whose equations can be written as Eqs. (14a) and (14b).

Because of Theorems 1 and 2 and their proof procedures, when the position-singularity curve in the characteristic plane is a set of hyperbolas, one of the two asymptotes of the hyperbolas must be parallel to the ridgeline. When the position-singularity curve in the characteristic plane is a pair of intersecting lines, one of the two intersecting lines must also be parallel to the ridgeline. Moreover, the equations of the two asymptotes of hyperbolas and the equations of the four pairs of intersecting lines must have the same form. Therefore, it can be concluded that the four pairs of intersecting lines are sure the degeneration of the sets of hyperbolas.

Some numerical examples are given to demonstrate the aforementioned results. Without special suffix, the geometry parameters of the mechanism are given as $R_b = 2$, $R_m = 1$, $\beta_b = 105°$, $\beta_m = 75°$. The moving platform and fixed one are two dissimilar semi-symmetrical hexagons. In addition, the orientation of the moving platform is given as $(60°, \theta, -45°)$ without special suffix, where θ is non-zero. The value of θ can be indeterminate because the geometric characteristics of the position-singularity locus in the characteristic plane is irrespective of θ. Coefficients a, b, d, e, and f varying with X_v for the aforementioned geometry and orientation parameters are expressed in Appendix B.

5.2.1. The cases of sets of hyperbolas. If $b \neq 0$ and $\Delta = 0$ for any given X_v, the position-singularity curve of the mechanism in the characteristic plane must be a set of hyperbolas. For instances, if $X_v = 1$, then $\delta = -603.43448$, $\Delta = -34165.75597$, and if $X_v = 2$, then $\delta = -443.98057$, $\Delta = -6854.35262$. Figure 5 shows the two hyperbolas for these given parameters.

The kinematic property of singularity can be analyzed using the method introduced in Section 3. For example, when $\theta = 30°$ and the other orientation and geometry parameters are given as aforementioned, these two sets of hyperbolas have particular points where all the segments associated with six extensible limbs of the mechanism intersect one common line. These particular singularities are of the type 5b as proposed by Merlet,[5–7] and can also be called the first special-linear-complex singularity (SLCS).[23] For this type of singularity, the unwanted instantaneous screw motions $\$^m$ are all pure rotations around the common intersecting line, and the pitch of the motion is equal to zero. The points of the first SLCS and the Plücker coordinates of common intersecting lines for orientation (60°, 30°, –45°) are given in Table I. The other points of hyperbolas belong to the type of Merlet 5a,[5–7], i.e. the general-linear-complex singularity (GLCS).[23] It can be shown that the mechanism may gain the same instantaneous screw motion on some different singularity points.

When $X_v = 2$, $x = 0.0127256$, $y = 1.2353741$, the configuration of the mechanism for orientation (60°, 30°, −45°) is shown in Fig. 6. The six line vectors associated with the six extensible limbs of the mechanism intersect a common line vector $\$^m$(0.4157354, −0.9044200, 0.0958567; 0.4217756, 0.0912636, −0.9681797), which is the reciprocal screw motion and can be obtained using

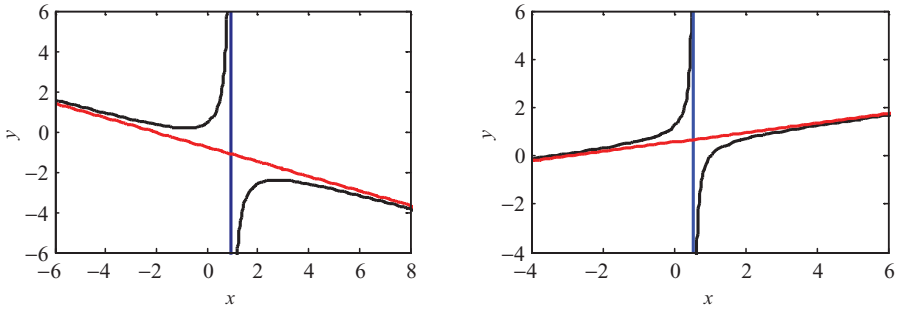

(a) $X_v = 1$ (b) $X_v = 2$

Fig. 5. (Colour online) Hyperbolas and their asymptotes for orientation $(60°, \theta, -45°)$ with two different X_v.

https://doi.org/10.1017/S0263574712000148 Published online by Cambridge University Press

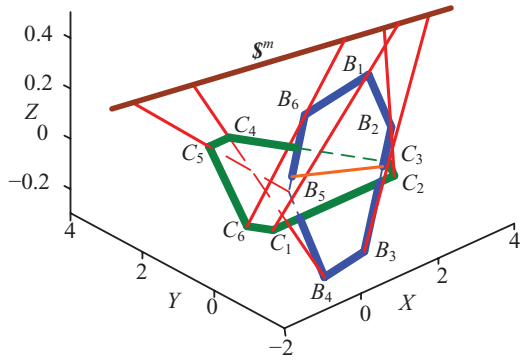

Fig. 6. (Colour online) One of the cases when all the segments intersect one common line.

Eq. (4). The pitch of the instantaneous screw motion $\$^m$, which can easily be calculated using Eq. (5), is equal to zero. Besides, Fig. 6 shows that the moving platform transverses the base one when the mechanism is in this special configuration, which is impossible in practice. When the mechanism is in the first SLCS, as shown in Table I, the all positions of the moving platform for orientation $(60^\circ, 30^\circ, -45^\circ)$ are graphically described in Fig. 7. When $X_\mathrm{v} = 1$ and $X_\mathrm{v} = 2$, it can be shown that both of the two cases have an impossible special configuration in practice as the moving platform transverses the base one.

5.2.2. The cases of four pairs of interesting lines. When the four roots of the equation $\Delta = 0$ with respect to X_v are all real and unequal to each other, Eq. (11) designates into four pairs of intersecting lines. Taking the geometry and orientation parameters as mentioned for example, the equation $\Delta = 0$ have four different and real roots $X_{\mathrm{v}\Delta j} (j = 1, 2, 3, 4)$ given in Appendix C. Then the four pairs of intersecting lines for these four different values of X_v are shown in Fig. 8.

When $\theta = 30^\circ$, the singularities belonging to the first SLCS can also be obtained as shown in Table II. Other singularity points are all the types of Merlet 5a,[5–7] i.e. the GLCS.[23]

5.2.3. The case of a parabola. Suppose $\delta = 0$, i.e. $b = 0$, then the solution of equation $b = 0$ with respect to X_v denoted as X_vb is easy to be achieved:

$$X_\mathrm{vb} = (\sqrt{6} + \sqrt{3} + \sqrt{2} + 1)t_2/2,$$

where $t_2 = \sqrt{8 - 2\sqrt{6} + 2\sqrt{2}}$ (the same below). In this case, Eq. (11) represents a curve of a parabola as shown in Fig. 9. The symmetry axis of the parabola must be parallel to the y-axis, i.e. the ridgeline.

The mechanism is always singular corresponding to the points lying in the parabola. When the moving platform locates at the three points for the orientation $(60^\circ, 30^\circ, -45^\circ)$, as shown in Table III, all the segments associated with the six limbs of mechanism can intersect one common line. This type of singularity belongs to the type of Merlet 5b or the first SLCS. Singularities of points lying in the parabola except these three points belong to the type of Merlet 5a, i.e. the GLCS.

5.2.4. The cases of two parallel lines or one line. As mentioned above, when $\phi = \pm 90^\circ$ and $\psi = \pm 90^\circ$, coefficients b and e of Eq. (11) are both identically vanishing. When $(\phi, \psi) = (90^\circ, -90^\circ)$, coefficients a, d, and f are deduced as shown in Appendix B. Substituting a, d, and f into expression "$d^2 - af$" gives

$$d^2 - af = \frac{729}{256}\big[24X_\mathrm{v}^2 + (42\sqrt{3} - 66 + 19\sqrt{6} - 57\sqrt{2})t_1 X_\mathrm{v} + 12\sqrt{3} - 32\sqrt{6} + 48\sqrt{2} + 56\big]^2. \tag{32}$$

So,

$$d^2 - af \geq 0.$$

If X_v satisfies inequalities $a \neq 0$ and $d^2 - af > 0$, Eq. (11) describes a pair of two lines, both of which are parallel to the y-axis, i.e. the ridgeline, and the equations of the two parallel lines can be expressed as

$$x = x_1 = \frac{-d + \sqrt{d^2 - af}}{a}, \tag{33a}$$

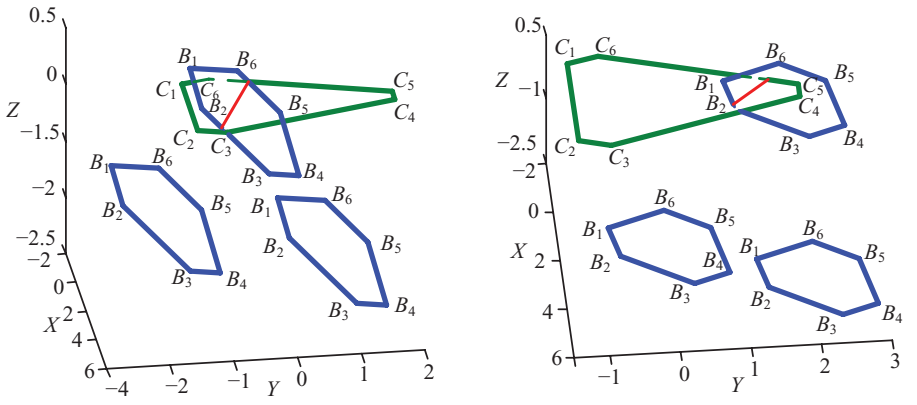

(a) $X_\mathrm{v} = 1$ (b) $X_\mathrm{v} = 2$

Fig. 7. (Colour online) Positions of the moving platform when the mechanism is in the first SLCS.

https://doi.org/10.1017/S0263574712000148 Published online by Cambridge University Press

Table II. Cases of the first SLCS of the four pairs of intersecting lines.

X_v	Line equation	(x, y)	$\$^m$
$X_{v\Delta1}$	$x = -e/b$	$(-e/b, -0.9530940)$	(0.0390977, 0.9790733, −0.1997167; 0.3796017, 0.5529974, 2.7852780)
		$(-e/b, 0.6806530)$	(0.4157354, −0.9044200, 0.0958566; 0.4217756, 0.0912636, −0.9681797)
		$(-e/b, 7.7672507)$	(0.8668142, 0.4289856, −0.2541743; 0.3633554, −0.8000619, −0.1111575)
	$abx + 2b^2y + 2bd - ae = 0$	ϕ	ϕ
$X_{v\Delta2}$	$x = -e/b$	$(-e/b, 10.0756856)$	(0.8668142, 0.4289855, −0.2541743; 0.3633554, −0.8000619, −0.1111575)
	$ab\,x + 2b^2\,y + 2bd - ae = 0$	$(-1.5696144, -0.3343702)$	(0.0390977, 0.9790733, −0.1997167; 0.3796017, 0.5529974, 2.7852780)
		$(-1.3551217, 0.4988792)$	(0.4157354, −0.9044200, 0.0958567; 0.4217756, 0.0912636, −0.9681797)
$X_{v\Delta3}$	$x = -e/b$	$(-e/b, 2.0487869)$	(0.4157354, −0.9044200, 0.0958567; 0.4217756, 0.0912636, −0.9681797)
	$abx + 2b^2y + 2bd - ae = 0$	$(6.5455278, -9.6073476)$	(0.8668142, 0.4289855, −0.2541743; 0.3633554, −0.8000619, −0.1111575)
		$(3.1378224, -5.6099630)$	(0.0390977, 0.9790733, −0.1997167; 0.3796017, 0.5529974, 2.7852780)
$X_{v\Delta4}$	$x = -e/b$	$(-e/b, -2.5233267)$	(0.0390977, 0.9790733, −0.1997167; 0.3796017, 0.5529974, 2.7852780)
	$abx + 2b^2y + 2bd - ae = 0$	$(-0.1607498, 1.1419691)$	(0.4157354, −0.9044200, 0.0958567; 0.4217756, 0.0912636, −0.9681797)
		$(1.5326338, 1.9087732)$	(0.8668142, 0.4289855, −0.2541743; 0.3633554, −0.8000619, −0.1111575)

Table III. Cases of the first SLCS of parabola.

(x, y)	$\$^m$
(−6.3573344, 20.0343964)	(0.8668142, 0.4289855, −0.2541743; 0.3633554, −0.8000619, −0.1111575)
(−3.9513612, 2.3348375)	(0.0390977, 0.9790733, −0.1997167; 0.3796017, 0.5529974, 2.7852780)
(−2.8115355, −0.2853030)	(0.4157354, −0.9044200, 0.0958567; 0.4217756, 0.0912636, −0.9681797)

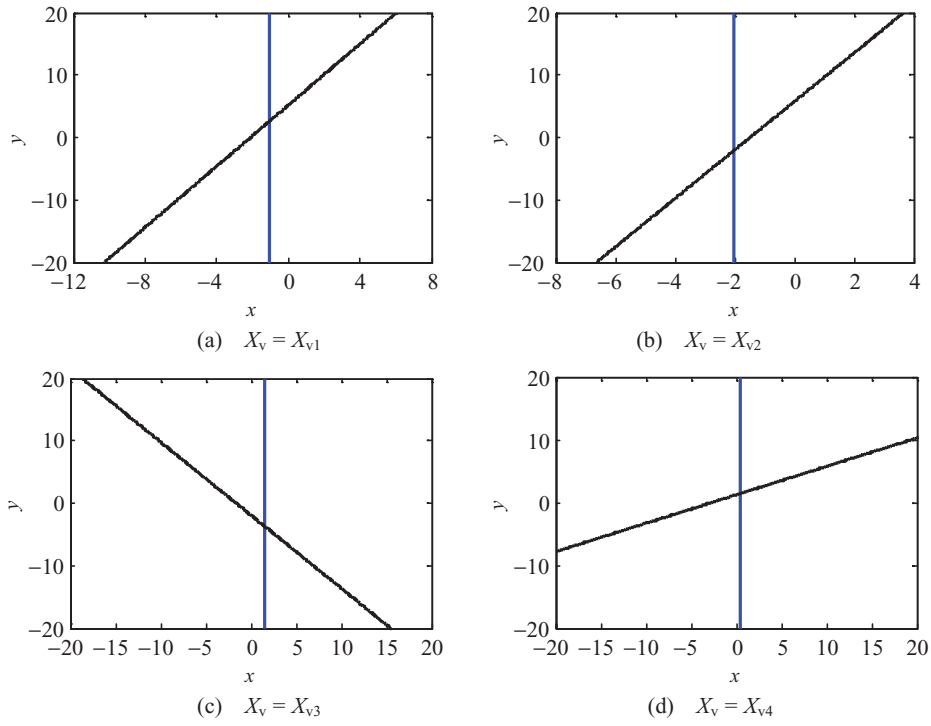

Fig. 8. (Colour online) Four pairs of intersecting lines.

https://doi.org/10.1017/S0263574712000148 Published online by Cambridge University Press

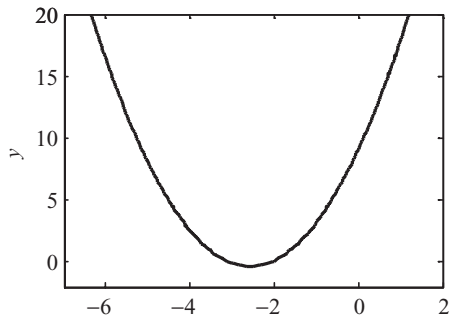

Fig. 9. Case of a parabola.

$$x = x_2 = \frac{-d - \sqrt{d^2 - af}}{a}. \tag{33b}$$

For examples, if $X_v = 0$ and $X_v = 1$, $d^2 - af = 12511.06705$ and $d^2 - af = 36.36808$, respectively. Figure 10 shows the two pairs of parallel lines, which represent the position-singularity loci lying in the characteristic plane for special orientation $(90°, \theta, -90°)$ when $X_v = 0$ or $X_v = 1$.

When $\theta = 30°$, further study shows that any singularity points on the lines $x = x_2$ for $X_v = 0$ and $X_v = 1$ are all the types of Merlet 5b, i.e. the first SLCS. Lines $x = x_1$ for both $X_v = 0$ and $X_v = 1$ have one singularity point of the type of Merlet 5b, i.e. the first SLCS. The results are shown in Table IV.

The two roots of equation $d^2 - af = 0$, which are denoted as X_{vl1} and X_{vl2}, respectively, can be solved:

$$X_{vl1} = -\frac{19}{48}\sqrt{6}t_1 + \frac{19}{16}\sqrt{2}t_1 - \frac{7}{8}\sqrt{3}t_1 + \frac{11}{8}t_1 + \frac{1}{24}\sqrt{1080 - 498\sqrt{2} + 270\sqrt{6} - 432\sqrt{3}}, \tag{34a}$$

$$X_{vl2} = -\frac{19}{48}\sqrt{6}t_1 + \frac{19}{16}\sqrt{2}t_1 - \frac{7}{8}\sqrt{3}t_1 + \frac{11}{8}t_1 - \frac{1}{24}\sqrt{1080 - 498\sqrt{2} + 270\sqrt{6} - 432\sqrt{3}}. \tag{34b}$$

Table IV. Cases of the first SLCS of two parallel lines.

X_v	(x, y)	$\$^m$
0	$(x_1, 0)$	(0, −0.9659258, 0.2588190; 0.8213398, 0, 0)
	$(x_2, 5)^*$	(−1, 0, 0; 0, 0.0879103, −1.4344416)
1	$(x_1, 1)$	(0, −0.9659258, 0.2588190; 0.8213398, 0, 0)
	$(x_2, 5)^*$	(1, 0, 0; 0, −0.1544102, 1.3192603)

*Only give one numeric example here to demonstrate the results, but it should be noticed that any singularity points on the line $x = x_2$ are the first SLCS.

Table V. Cases of the first SLCS of one line.

X_v	(x, y)	$\$^m$
X_{vl1}	$(-d/a, 10)$	(1, 0, 0; 0, 1.0597090, 3.4221765)
X_{vl2}	$(-d/a, 10)$	(−1, 0, 0; 0, 0.1668163, −1.2977724)

When $X_v = X_{vl1}$ or $X_v = X_{vl2}$, Eq. (34a) is equivalent to Eq. (34b), and these two equations represent the same line $x = -d/a$ as shown in Fig. 11.

When $X_v = X_{vl1}$ or $X_v = X_{vl2}$, it can be further found that any singularity point lying in the line, $x = -d/a$, belongs to the type of Merlet 5b, i.e. the first SLCS. The unwanted instantaneous motion $\$^m$ can also be deduced using the method as mentioned in Section 3. Two singularity points and their corresponding unwanted instantaneous motions are given here as examples, as shown in Table V.

With above presentation, when θ is non-zero, the geometric characteristics and kinematic property of the position-singularity loci of the mechanism in the characteristic planes for given orientations are analyzed. In addition, the mechanism may gain the same unwanted instantaneous screw motion on some different singular configurations.

5.3. Position-singularity locus when $\theta = 0$

When $\theta = 0$, the moving platform parallel to the base one. Meanwhile, simplifying each term of the matrix $[\boldsymbol{D}]$ using the trigonometric formula and then expanding the determinant of matrix $[\boldsymbol{D}]$ can yield the following equation:

$$\cos(\phi + \psi)Z^3 = 0. \tag{35}$$

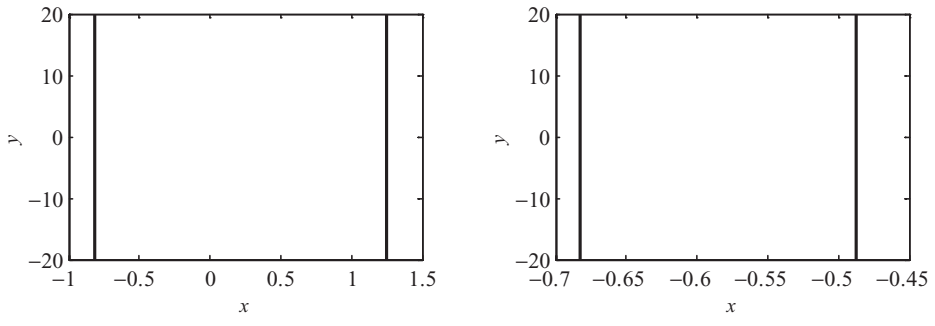

(a) $X_v = 0$ (b) $X_v = 1$

Fig. 10. Cases of two parallel lines for two different X_v.

https://doi.org/10.1017/S0263574712000148 Published online by Cambridge University Press

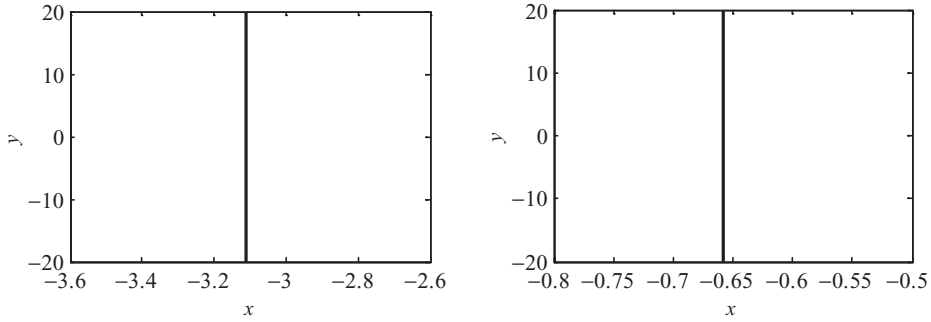

(a) $X_v = X_{vl1}$ (b) $X_v = X_{vl2}$

Fig. 11. The cases of one line parallel to the y-axis.

(1) When $Z = 0$, the moving platform is coincident to the base one and the mechanism is singular. In this special configuration, the mechanism has 2-DOF for rotation and 1-DOF for translation. The Plücker coordinates of the three unwanted instantaneous motions are (1, 0, 0; 0, 0, 0), (0, 1, 0; 0, 0, 0), and (0, 0, 0; 0, 0, 1). It can be shown that one of the 2-DOF for rotation is around the x-axis and another is around the y-axis, and the 1-DOF for translation is along the z-axis.
(2) When $(\phi + \psi) = \pm 90^\circ$, it is the type of singularity proposed by Fichter[4] and belongs to the type of Merlet 5a, i.e. the GLCS. The unwanted instantaneous screw motion can also be calculated using the methods introduced in Section 3.

6. Conclusions

For the special class of Stewart parallel mechanisms with two dissimilar semi-symmetrical hexagons, the position-singularity locus of the mechanism for a constant-orientation is extremely complicated; besides, the geometric characteristics of the position-singularity locus lying in a general oblique plane are very difficult to be identified. However, the position-singularity curves in the characteristic plane, where the moving platform lies, can easily be characterized, and then some meaningful results can be obtained as follows:

(1) When θ is non-zero, the position-singularity locus of the mechanism for a constant-orientation is stacked with infinitely many curves of the second order, which are generally infinitely many sets of hyperbolas, four pairs of intersecting lines, and a hyperbola. For special orientations $(\pm 90^\circ, \theta, \pm 90^\circ)$, the quadratic curve in an arbitrary characteristic plane can degenerate into two parallel lines or even one line, all of which are parallel to the ridgeline.
(2) In particular, the equations of the asymptotes of hyperbolas and equations of the four pairs of intersecting lines have the same forms. Besides, one of the two asymptotes and one of the two intersecting lines must be parallel to the ridgeline. Hence, the four pairs of intersecting lines are the degeneration of hyperbolas. Two theorems involving these results are proposed and proved.
(3) All of the position-singularity curves in the characteristic planes have the singularity points of the type of Merlet 5b, i.e. the first SLCS, where all of the lines associated with the six limbs intersect one common line simultaneously, and the unwanted instantaneous screw motion is a pure rotation around the common line. Especially, when the quadratic position-singularity curves degenerate into two parallel lines and even one line, which are all parallel to the ridgeline, any singularity point on one of the lines are the type of Merlet 5b, i.e. the first SLCS.
(4) When θ is zero, the expression of the position-singularity locus is simpler than the position-singularity locus with θ being non-zero. In this case, two main types of singularities, whose kinematic property can also be obtained, are known to the researchers.

In this paper, after analyzing the singularity curves in the series of characteristic planes, the geometric characteristics and kinematic property of the singularity locus for a constant-orientation are addressed. This work has great significance on the design of this special class of mechanisms. According to the results, the designers determine whether and how the singularity can be avoided within the workspace for a given orientation. Our current work is focusing on developing the algorithms for determining the nonsingular position-workspace of mechanism for a given orientation based on research findings.

Acknowledgments

The research work reported here is supported by the National Natural Science Foundation of China under Grant No. 50905075, the Self-determined Research Program of Jiangnan University under Grant No. JUSRP10908, the Funds for Anhui Province Young Talent of Colleges and Universities under Grant No. 2010SQRL047ZD, Jiangsu Province Graduate Research and Innovation Program of China under Grant No. CXZZ11_0482, the Open Project of Jiangsu Province Digital Manufacturing Technology Key Laboratory under Grant No. HGDML-0910, the Open Project of the State Key Laboratory of Fluid Power and Mechatronic Systems under Grant No. GZKF-201105, the Doctoral Science Foundation of Jiangnan University under Grant No. JUDCF11014, as well as the Funds for Youth Scholars of Anhui University of Science and Technology under Grant No. QN200822.

https://doi.org/10.1017/S0263574712000148 Published online by Cambridge University Press

References

1. D. Stewart, "A platform with six degrees of freedom," *Proc. Inst. Mech. Eng.* **180**(5), 371–378 (1965).
2. Z. Huang, Y. S. Zhao and T. S. Zhao, *Advanced Spatial Mechanism* (Higher Education Press, Beijing, China, 2005).
3. K. H. Hunt, "Structural kinematics of in-parallel-actuated-robot-arms," *ASME, J. Mech. Transm. Autom. Des.* **105**(4), 705–712 (1983).
4. E. F. Fichter, "A Stewart platform-based manipulator: General theory and practical construction," *Int. J. Robot. Res.* **5**(2), 157–182 (1986).
5. J. P. Merlet, "Parallel Manipulator Part 2: Singular Configurations and Grassmann Geometry," *Technical Report* No.791 (INRIA, Centre de Sophia Antipolis, Valbonne, France, 1988) 194–212.
6. J. P. Merlet, "Singular configurations of parallel manipulators and Grassmann geometry," *Int. J. Robot. Res.* **8**(5), 45–56 (1989).
7. J. P. Merlet, "Singular Configuration and Direct Kinematics of a New Parallel Manipulator," **In**: *Proceedings of the IEEE International Conference on Robotics and Automation*, Nice, France (1992) pp. 338–343.
8. C. M. Gosselin and J. Angeles, "Singularity analysis of closed-loop kinematic chains, " *IEEE Trans. Robot. Autom.* **6**(3), 281–290 (1990).
9. D. Zlatanov, R. G. Fenton and B. Benhabib, "Singularity Analysis of Mechanisms and Robots via a Motion-Space Model of the Instantaneous Kinematics," **In**: *Proceedings of the IEEE International Conference on Robobics and Automation*, San Diego, USA (1994) 980–991.
10. O. Ma and J. Angeles, "Architecture Singularity of Platform Manipulators," **In**: *Proceedings of the IEEE International Conference on Robotics and Automation*, Sacramento, USA (1991) 1542–1547.
11. Z. Huang, Y. S. Zhao, J. Wang *et al.*, "Kinematic principle and geometrical condition of general-linear-complex special configuration of parallel manipulators," *Mech. Mach. Theory* **34**(8), 1171–1186 (1999).
12. Z. Huang and X. Du, "General-linear-complex special configuration analysis of 3/6-SPS Stewart parallel manipulator," *China Mech. Eng.* **10**(9), 997–1000 (1999).
13. Z. Huang, L. Chen and Y. W. Li, "The singularity principle and property of Stewart parallel manipulator," *J. Robot. Syst.* **20**(4), 163–176 (2003).
14. J. Saglia, J. S Dai and D. G. Caldwell, "Geometry and kinematic analysis of a redundantly actuated parallel mechanism that eliminates singularity and improves dexterity," *ASME, J. Mech. Des.* **130**(12), 124501_1–5 (2008).
15. H. Pendar, M. Mahnama and H. Zohoor, "Singularity analysis of parallel manipulators using constraint plane method," *Mech. Mach. Theory* **1**(46), 33–43 (2011).
16. S. J. Zhu, Z. Huang and M. Y. Zhao, "Singularity analysis for six practicable 5-DoF fully symmetrical parallel manipulators," *Mech. Mach. Theory* **4**(44), 710–725 (2009).
17. P. Ben-Horin and M. Shoham, "Singularity analysis of a class of parallel robots based on Grassmann–Cayley algebra," *Mech. Mach. Theory* **8**(41), 958–970 (2006).
18. H. Li, C. M. Gosselin, M. J. Richard and B. Mayer St-Onge, "Analytic form of the six-dimensional singularity locus of the general Gough–Stewart platform," *ASME, J. Mech. Des.* **1**(128), 279–287 (2006).
19. J. Sefrioui and C. M. Gosselin, "Study and representation of the singularities of spheric parallel manipulators with prismatic actuators, with three degrees of freedom," *Mech. Mach. Theory* **29**(4), 559–579 (1994).
20. J. Sefrioui and C. M. Gosselin, "On the quadratic nature of the singularity curves of planar three-degree-of-freedom parallel manipulators," *Mech. Mach. Theory* **30**(4), 533–551 (1995).
21. J. Wang and C. M. Gosselin, "Kinematic analysis and singularity loci of spatial four-degree-of-freedom parallel manipulators using a vector formulation," *ASME, J. Mech. Des.* **120**(4), 555–558 (1998).
22. B. M. St-Onge and C. M. Gosselin, "Singularity analysis and representation of the general Gough–Stewart platform," *Int. J Robot. Res.* **19**(3), 271–288 (2000).
23. Z. Huang, Y. Cao, Y. W. Li and L. H. Chen, "Structure and property of the singularity loci of the 3/6-Stewart–Gough platform for general orientations," *Robotica* **1**(24), 75–84 (2006).
24. Z. Huang and Y. Cao. "Property identification of singularity loci of a class of the Gough–Stewart manipulators," *Int. J. Robot. Res.* **24**(8), 675–685 (2005).
25. S. Bandyopadhyay and A. Ghosal, "Geometric characterization and parametric representation of the singularity manifold of a 6–6 Stewart platform manipulator," *Mech. Mach. Theory* **11**(41), 1377–1400 (2006).
26. S. Cheng, H. Wu and C. Wang *et al.*, "A novel method for singularity analysis of the 6-SPS parallel mechanisms," *Sci. China:Technol. Sci.* **54**(5), 1220–1227 (2011).
27. G. Nawratil, "Stewart–Gough platforms with non-cubic singularity surface," *Mech. Mach. Theory* **12**(45), 1851–1863 (2009).

Appendix A

$$
\begin{aligned}
&\boldsymbol{B}_1' : (-R_\mathrm{m}\cos(30^\circ+\beta_\mathrm{m}/2), -R_\mathrm{m}\sin(30^\circ+\beta_\mathrm{m}/2), 0)\\
&\boldsymbol{B}_2' : (R_\mathrm{m}\cos(30^\circ+\beta_\mathrm{m}/2), -R_\mathrm{m}\sin(30^\circ+\beta_\mathrm{m}/2), 0)\\
&\boldsymbol{B}_3' : (R_\mathrm{m}\cos(30^\circ-\beta_\mathrm{m}/2), -R_\mathrm{m}\sin(30^\circ-\beta_\mathrm{m}/2), 0)\\
&\boldsymbol{B}_4' : (R_\mathrm{m}\sin(\beta_\mathrm{m}/2), R_\mathrm{m}\cos(\beta_\mathrm{m}/2), 0)\\
&\boldsymbol{B}_5' : (-R_\mathrm{m}\sin(\beta_\mathrm{m}/2), R_\mathrm{m}\cos(\beta_\mathrm{m}/2), 0)\\
&\boldsymbol{B}_6' : (-R_\mathrm{m}\cos(30^\circ-\beta_\mathrm{m}/2), -R_\mathrm{m}\sin(30^\circ-\beta_\mathrm{m}/2), 0)\\
&\boldsymbol{C}_1 : (-R_\mathrm{b}\sin(\beta_\mathrm{b}/2), -R_\mathrm{b}\cos(\beta_\mathrm{b}/2), 0)\\
&\boldsymbol{C}_2 : (R_\mathrm{b}\sin(\beta_\mathrm{b}/2), -R_\mathrm{b}\cos(\beta_\mathrm{b}/2), 0)\\
&\boldsymbol{C}_3 : (R_\mathrm{b}\cos(30^\circ-\beta_\mathrm{b}/2), R_\mathrm{b}\sin(30^\circ-\beta_\mathrm{b}/2), 0)\\
&\boldsymbol{C}_4 : (R_\mathrm{b}\cos(30^\circ+\beta_\mathrm{b}/2), R_\mathrm{b}\sin(30^\circ+\beta_\mathrm{b}/2), 0)\\
&\boldsymbol{C}_5 : (-R_\mathrm{b}\cos(30^\circ+\beta_\mathrm{b}/2), R_\mathrm{b}\sin(30^\circ+\beta_\mathrm{b}/2), 0)\\
&\boldsymbol{C}_6 : (-R_\mathrm{b}\cos(30^\circ-\beta_\mathrm{b}/2), R_\mathrm{b}\sin(30^\circ-\beta_\mathrm{b}/2), 0)
\end{aligned}
$$

Appendix B

When $(\phi, \psi) = (60^\circ, -45^\circ)$, and $R_\mathrm{b} = 2$, $R_\mathrm{m} = 1$, $\beta_\mathrm{b} = 105^\circ$, and $\beta_\mathrm{m} = 75^\circ$, coefficients a, b, d, e, and f of Eq. (11) are all functions of X_v and determined by the following equations:

$$
\begin{aligned}
a &= -\frac{27}{8}\sqrt{2}(\sqrt{3}+1)[(3\sqrt{6}-5\sqrt{3}-5\sqrt{2}+7)t_2 + 2X_\mathrm{v}],\\
b &= \frac{27}{16}\sqrt{2}(\sqrt{3}-1)[(\sqrt{6}+\sqrt{3}+\sqrt{2}+1)t_2 - 2X_\mathrm{v}],\\
d &= \frac{27}{32}\sqrt{2}(\sqrt{3}-1)[-20-4\sqrt{3}+8\sqrt{2}\\
&\quad +14\sqrt{6}+(8-9\sqrt{2}+3\sqrt{3})t_2X_\mathrm{v} - 8X_\mathrm{v}^2],\\
e &= \frac{9}{64}t_2(-3\sqrt{2}-2\sqrt{3}+3\sqrt{6}+6)[\big(3-5\sqrt{3}+\sqrt{6}\\
&\quad -3\sqrt{2})t_2 + 6X_\mathrm{v}],\\
f &= \frac{27}{32}t_2(-3\sqrt{2}-2\sqrt{3}+\sqrt{6}+2)[-6\sqrt{3}+4\sqrt{2}\\
&\quad +2\sqrt{6}+6+(4-3\sqrt{2}-3\sqrt{3})t_2X_\mathrm{v} + 4X_\mathrm{v}^2].
\end{aligned}
$$

When $(\phi, \psi) = (90^\circ, -90^\circ)$, b and e are both constant zero. Coefficients a, d, and f of Eq. (11) can be deduced as

https://doi.org/10.1017/S0263574712000148 Published online by Cambridge University Press

follows:

$$a = -\frac{9\sqrt{3}}{2}[(3\sqrt{3} - 6\sqrt{2} + 2\sqrt{6} - 6)t_1 + 6X_{\mathrm{v}}],$$

$$d = -\frac{81}{2}X_{\mathrm{v}}^2 - \left(\frac{459}{16}\sqrt{6} + \frac{513}{8}\sqrt{3} - \frac{1377}{16}\sqrt{2} - \frac{729}{8}\right)t_1 X_{\mathrm{v}} + 54(\sqrt{6} - \sqrt{2}) - \frac{27}{4}\sqrt{3} - \frac{135}{2},$$

$$f = -\frac{9t_1}{64}(2\sqrt{3} + \sqrt{6} - \sqrt{2} - 2)[6X_{\mathrm{v}} + (2\sqrt{6} + \sqrt{3} - 3\sqrt{2} - 6)t_1][12X_{\mathrm{v}} + (5\sqrt{6} + 14\sqrt{3} - 15\sqrt{2} - 18)t_1].$$

Appendix C

When $(\phi, \psi) = (60^\circ, -45^\circ)$, and $R_{\mathrm{b}} = 2$, $R_{\mathrm{m}} = 1$, $\beta_{\mathrm{b}} = 105^\circ$, and $\beta_{\mathrm{m}} = 75^\circ$, the solutions of equation $\Delta = -ae^2 - b^2 f + 2bde = 0$ are denoted as $X_{\mathrm{v}\Delta j}(j = 1, 2, 3, 4)$ and can be derived as follows:

$$X_{\mathrm{v}\Delta 1} = \frac{1}{2}(\sqrt{6} + 1)t_2,$$

$$X_{\mathrm{v}\Delta 2} = \frac{2}{3}t_3 \sin\left(-\frac{1}{3}\arctan\frac{t_4}{t_2 t_5} + \frac{\pi}{6}\right) + \frac{1}{12}(4\sqrt{3} + \sqrt{6} - \sqrt{2} + 2)t_2,$$

$$X_{\mathrm{v}\Delta 3} = -\frac{1}{3}t_3 \sin(-\frac{1}{3}\arctan\frac{t_4}{t_2 t_5} + \frac{\pi}{6}) - \frac{\sqrt{3}}{3}t_3 \times \sin\left(\frac{1}{3}\arctan\frac{t_4}{t_2 t_5} + \frac{\pi}{3}\right) + \frac{1}{12}(4\sqrt{3} + \sqrt{6} - \sqrt{2} + 2)t_2,$$

$$X_{\mathrm{v}\Delta 4} = -\frac{1}{3}t_3 \sin\left(-\frac{1}{3}\arctan\frac{t_4}{t_2 t_5} + \frac{\pi}{6}\right) + \frac{\sqrt{3}}{3}t_3 \times \sin\left(\frac{1}{3}\arctan\frac{t_4}{t_2 t_5} + \frac{\pi}{3}\right) + \frac{1}{12}(4\sqrt{3} + \sqrt{6} - \sqrt{2} + 2)t_2,$$

where

$$t_3 = (9956 + 5040\sqrt{6} + 1274\sqrt{2} - 480\sqrt{3})^{1/6},$$

$$t_4 = 6 \cdot (22744 + 1446\sqrt{2} - 576\sqrt{3} + 2352\sqrt{6})^{1/6},$$

$$t_5 = 83 - 81\sqrt{2} + 56\sqrt{6} - 103\sqrt{3}.$$

https://doi.org/10.1017/S0263574712000148 Published online by Cambridge University Press